GEOMETRIC INTEGRATION AND ITS APPLICATIONS

C.J. Budd[1] and M.D. Piggott[2]

Abstract

This paper aims to give an introduction to the relatively new field of geometric integration. During the course of looking at a series of examples, ideas and techniques are introduced. Effective numerical methods for challenging problems are described. These methods aim to preserve certain geometric structures inherent in the underlying problem such as symplecticity, conservation laws and Lie group symmetries.

KEY WORDS: Numerical methods, qualitative behaviour, Hamiltonian systems, singularity capturing, meteorology, frontogenesis.

1 Introduction

The modern study of natural phenomena described by ordinary or partial differential equations usually requires a significant application of computational effort and to understand the design and operation of computer algorithms, numerical analysis is essential. A huge amount of effort over the past fifty years (and earlier) has thus been applied to the research of numerical methods for differential equations. This research has led to many ingenious algorithms and associated codes for the computation of solutions to such differential equations. Most of these algorithms are based upon the natural technique of discretising the equation in such a way as to keep the local truncation errors associated with the discretisation as small as possible. The resulting discrete systems are then solved with carefully designed linear and nonlinear solvers. When coupled with effective error control strategies these methods can often lead to very accurate solutions of the associated differential equations, provided that the times for integration are not long and the solution remains reasonably smooth.

However, methods based on the analysis of local truncation errors do not necessarily respect, or even take into account, the qualitative and global features of the problem or equation. It can be argued that in some situations these global structures tell us more about the underlying problem than the local information given by the expression of the problem in terms of differentials. The recent growth of geometric integration has, in contrast, led to the development of numerical methods which systematically incorporate

[1]Dept. of Mathematical Sciences, University of Bath, Claverton Down, Bath, BA2 7AY, UK. cjb@maths.bath.ac.uk

[2]Dept. of Mathematical Sciences, University of Bath, Claverton Down, Bath, BA2 7AY, UK. mapmdp@maths.bath.ac.uk

qualitative information of the underlying problem into thier structure. As it is often unclear a-priori what the correct qualitative features of a problem are (and it is highly unlikely that one numerical method can preserve all of them), geometric integration necessarily involves a dialogue between numerical analysts, applied mathematicians, engineers and scientists.

Some of the above comments may be exemplified by the following diagram. Given a differential equation which we seek to approximate using a numerical method, the left hand side of the diagram represents the use of classical method of approximating the equation, whereas the right hand side displays the geometric integration philosophy.

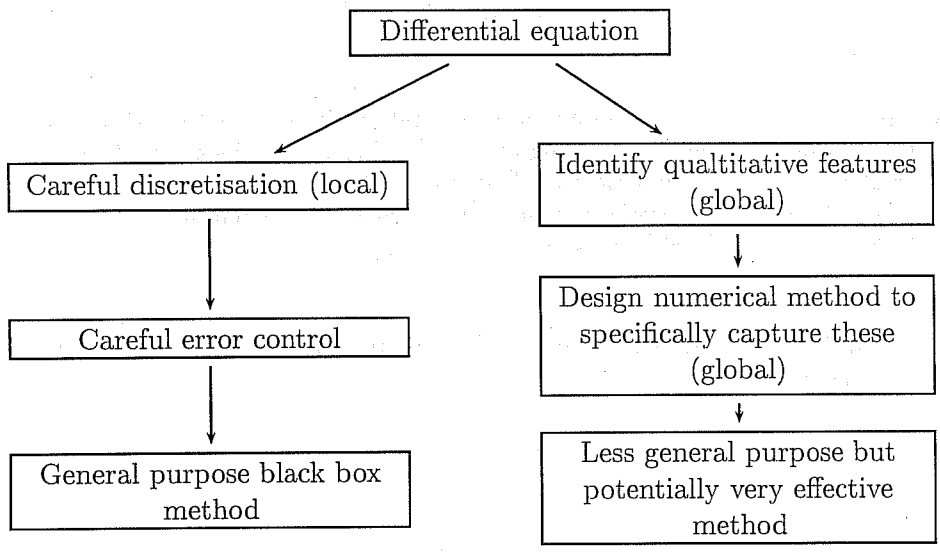

The aim of this paper is to introduce and explain, some ideas, methods, and techniques used in the field of geometric integration, basing our discussion around several carefully chosen examples. We further aim to discuss how some of the mentioned ideas could be used in problems arising in the fields of meteorology and numerical weather prediction. This discussion is necessarily incomplete and further details of geometric integration can be found in the recent reviews and discussions listed in the following references [5, 29, 18, 7].

The remainder of this paper is organised as follows. In Section 2 we present an, obviously not exhaustive, description of some of the qualitative properties of differential equations and problems that we have in mind. In Section 3 we review some model problems, and suitable geometric integration based numerical methods, which currently appear in the geometric integration literature. In Section 4 we look ahead to some model problems arising in meteorology for which geometric based ideas can be beneficial. We briefly discuss what possible impacts geometric integration could have on their computational analysis. Finally, in section 5 we present some concluding remarks.

2 Qualitative properties

In this section we shall briefly look at some of the qualitative and global features of a system described by a differential equation which we have in mind when we talk about

geometric integration. The discussions of such qualitative features will, out of necessity (and the vast complexity of possible behaviours of solutions of differential equations), be very brief and introductory. We shall wherever possible include references to material where much further information may be found.

2.1 A Partial Listing

There are many possible qualitative features which may be present in the systems modelled by ordinary or partial differential equations. We shall not attempt to give a complete listing, however below we give a partial listing which covers a wide variety of possibilities and mention how the different qualitative properties may be linked to one another.

1. *Conservation laws* Underlying many systems are conservation laws. These may include the conservation of total quantities (usually integrals over the domain in which the system evolves) such as mass, energy and momentum, or instead quantities which are conserved along particle trajectories and flows such as fluid density or potential vorticity. The loss of energy in a system describing planetary motion will inevitably lead to the planet so modelled spiralling into the sun, which is clearly incorrect qualitatively. Similarly it is widely accepted [14] that in large scale modelling of the oceans and atmosphere it is essential to conserve potential vorticty to retain the overall qualitative dynamics of the solution. The above are conservation laws associated directly with the solution, however, for Hamiltonian problems we may also have the conservation of symplectic structures in phase space and volume preservation in divergence-free systems which are conservation laws associated with the phase space in which the solution is posed. (They are of course related, for example the Hamiltonian of the solution is conserved in autonomous Hamiltonian systems.)

2. *Symmetries* Many systems are invariant under the actions of symmetries and may also have solutions (self-similar solutions) which do not change when the symmetry group acts. The possible symmetries may include the following

   - *Galilean symmetries* such as translations, reflexions and rotations. One of the key problems in computer vision is to recognise an object which may be a translation or rotation of a known pattern. One way to do this is to associate invariants to the object (such as curvature) which do not change under the action of a Galilean symmetry [31]. The study of the motion of rigid bodies in three-dimensional space (such as a satellite or a robot arm) is dominated by the fact that such systems are invariant under Galilean symmetries [26].
   - *Scaling symmetries* Many physical problems have the property that they are invariant under rescalings in either time or space (this partly reflects the fact that the laws of physics should not depend upon the units in which they are measured [2].) An example of this is Newton's law of gravitation which is invariant under a rescaling in time and space. This invariance leads directly to Kepler's third law linking the period of an elliptical periodic orbit to the length of the major axis of the ellipse — determining this law does not involve solving the differential equation.
   - *Lie group symmetries* These are deeper symmetries than those described above, often involving the invariance of the system to a (nonlinear) Lie group of transformations. An important example (which arises naturally in mechanics) is the invariance of a system to the action of the rotation group $SO(3)$. An excellent discussion of such symmetries is given in [31]. The review article [25] describes

the numerical approach to computing solutions of ordinary differential equations with such symmetries.

3. *Asymptotic behaviours* The differential system under study may evolve in time so that over a long time its dynamics in some sense simplifies. For example it may ultimately evolve so that its dynamics is restricted to a low dimensional attractor. Complex structures starting from arbitrary initial data may simplify into regular patterns [17]. Alternatively, the equation may have solutions which form singularities in finite time such as weather fronts (derivative singularities) or combustion in which the solution itself becomes singular at a single point.

4. *Orderings in the solutions* The differential equation may possess some form of maximum principle which leads to a preservation of the solution orderings. For example, given two sets of initial data $u_0(x)$ and $v_0(x)$ for a partial differential equation, the solutions may respect the ordering that if $u_0(x) < v_0(x)$ for all x, then $u(x,t) < v(x,t)$ for all x and t. The linear heat equation $u_t = u_{xx}$ has this property. A related concept is that of solution convexity. Indeed, the preservation of the convexity of a pressure function across a front is an important feature of numerical weather prediction [11].

It is important to realise that these global properties may be closely linked to one another. For example, if the differential equation is derived from a variational principle linked to a Lagrangian function then, via Noether's theorem [31], each continuous symmetry of the Lagrangian leads directly to a conservation law for the underlying equation. This has a beautiful application to numerical analysis. If a numerical method is also based upon a Lagrangian and this Lagrangian has symmetries then the numerical method automatically has a discrete conservation law associated with this symmetry [16]. Symmetry when coupled with solution orderings frequently leads to an understanding of the asymptotic behaviour of the equation. In particular, self-similar solutions (which are invariant under the group actions) can be used to bound the actual solution from above and below. The solution behaviour is then constrained to follow that of the self-similar solution [33]. Singularities in the equation often have more *local* symmetry than the general solution of the equation because the effects of boundary and intial conditions are less important [2].

Some natural questions to ask of a numerical method which attempts to emulate some of these properties are as follows. What is the benefit (if any) of designing numerical methods which take into account qualitative properties of the underlying solution? For systems which possess more than one important qualitative property, how much of this structure can we hope to preserve? Which qualitative properties turn out to be more important, or beneficial, from a computational viewpoint?

2.2 Why preserve structure?

There are several reasons why it is worthwhile to preserve qualitative structure. Firstly, many of the above properties can be found in systems which occur naturally in applications. For example, large scale molecular or stellar dynamics can be described by Hamiltonian systems with many conservation laws. Mechanical systems evolve under rotational constraints, as do many of the probles of fluid mechanics. Partial differential equations possessing scaling symmetries and self-similarity arise in fluid and gas dynamics, combustion, nonlinear diffusion and mathematical biology. Partial differential equations with a

Hamiltonian structure are important in the study of solitons (such as the KdV and nonlinear Schrödinger equation) and the semi-geostrophic equations in meteorology also have a Hamiltonian structure. The list could be virtually endless.

In designing our numerical method to preserve some structure we hope to see some improvements in our computations. For a start we will be studying a discrete dynamical system which has the same properties as the continous one, and thus can be thought of as being in some sense close to the underlying problem in that stability properties, orbits and long-time behaviour may be common to both systems. Geometric structures often (as we shall see) make it easier to estimate errors, and in fact local and global errors may well be smaller for no extra computational expense. Geometric integration methods designed to capture specific qualitative properties may also preserve additional properties of the solution *for free*. For example symplectic methods for Hamiltonian problems have excellent energy conservation properties and can conserve angular momentum or other invariants (which may not even be known in advance).

In conclusion geometric integration methods (including Lie group methods, sympletic integrators, splitting methods, certain adaptive methods, etc.) can often 'go where other methods cannot'. They have had success in the accurate computation of singularities, long-term integration of the solar system, analysis of highly oscillatory systems (quantum physics for example). The list of application areas keeps on growing.

3 Case studies I: standard model problems

We now present some case studies to illustrate some of the underlying methods as applied to both ordinary and partial differential equations. In these case studies we aim to show both the power of the new methods and to indicate areas for future developement. The case studies will be as follows

1. Planetary motion and molecular dynamics : Here we see geometric integration applied to a set of Hamiltonian ordinary differential equations.
2. Mechanical systems : These are systems with rotational symmetry with momentum and energy conservation.
3. Scale invariant systems and global error estimates.
4. Singularity capturing (via an adaptive approach) in partial differential equations.

In section 4 we will look at two meteorological problems: The prediction of large scale atmospheric phenomena, including fronts, using the semi-geostrophic equations; and ensemble prediction using singular value decomposition (SVD).

3.1 Hamiltonian systems

Some of the earliest major work in geometric integration centred on the development of *symplectic* methods for Hamiltonian systems of ordinary differential equations, see [34]. We now present a quick introduction to some of the underlying ideas and notation.

Consider a mechanical system with generalised coordinates $\mathbf{q} \in \mathbb{R}^d$ and Lagrangian $L = T - U$, where $T \equiv T(\mathbf{q}, \dot{\mathbf{q}})$ represents the kinetic energy of the system and $U \equiv U(\mathbf{q})$ its potential energy. It can be shown that the dynamics of such a system are given by

the solution of a variational problem, which can in turn be written as the solution of the following Euler-Lagrange equations

$$\frac{d}{dt}\left(\frac{\partial L}{\partial \dot{\mathbf{q}}}\right) - \frac{\partial L}{\partial q} = 0. \tag{1}$$

Hamilton introduced new variables $\mathbf{p} = \partial L/\partial \dot{\mathbf{q}} \in \mathbb{R}^d$, the conjugate generalized momenta of the system. He further defined the Hamiltonian as $H(\mathbf{p}, \mathbf{q}) = \mathbf{p}^T\dot{\mathbf{q}} - L(\mathbf{q}, \dot{\mathbf{q}})$ and showed that (1) is equivalent to the following system of $2d$ first order equations, we call them Hamilton's equations

$$\begin{aligned} \dot{\mathbf{p}} &= -\frac{\partial H}{\partial \mathbf{q}}, \\ \dot{\mathbf{q}} &= \frac{\partial H}{\partial \mathbf{p}}. \end{aligned} \tag{2}$$

This is called the *canonical form* for a Hamiltonian system. Presently we shall extend our definition of such systems. Note that for our considered mechanical system $H \equiv T + U$ and thus the Hamiltonian represents the total energy present.

Further details may be found in [1, 26, 31], and for a numerical viewpoint see [34, 21].

We now move a little into abstraction and consider arbitrary Hamiltonian systems which do not necessarily arise from a mechanical system. It is a simple exercise to show that a time independent Hamiltonian is a first integral (or conserved quantity) of the dynamics described by (2). We now discuss a further property of Hamiltonian systems — the preservation of the symplectic structure, or symplecticity of the flow.

A flow, or mapping, is called symplectic if it preserves the differential 2-form $d\mathbf{p} \wedge d\mathbf{q}$. This form, applied to two vectors in $\mathbb{R}^d$, can be thought of as representing the sum of the oriented areas of projections onto coordinate planes of the parallelogram spanned by the two vectors. For the case $d = 1$ this simply reduces to two-dimensional area, and hence a symplectic mapping is simply an area preserving map. Poincaré proved that the flow of any Hamiltonian system has this symplecticity property. It is further possible to show that symplecticity of the flow of a differential system is equivalent to the system being Hamiltonian. Thus the symplecticity property is much stronger than simple preservation of $2d$-dimensional volume, since Hamiltonian systems preserve volume (Liouville's theorem) but it is possible to find volume preserving systems which are not Hamiltonian.

We shall call a numerical one-step method for (2) symplectic if, when applied to a smooth Hamiltonian system, the discrete mapping defined by the mapping is symplectic. A simple example of such a method is the implicit midpoint rule, which for $\dot{\mathbf{u}} = \mathbf{f}(\mathbf{u})$ takes the form

$$\mathbf{u}_{n+1} = \mathbf{u}_n + \Delta t\, \mathbf{f}\left(\frac{1}{2}(\mathbf{u}_n + \mathbf{u}_{n+1})\right).$$

3.1.1 Molecular or stellar dynamics and some numerical methods

The classical equations for a system of N particles (or heavenly bodies) interacting via a potential force V can be written in Hamiltonian form (2), with the Hamiltonian function given by

$$H(p, q) = \frac{1}{2}\sum_{i=1}^{N} m_i^{-1} p_i^T p_i + \sum_{i<j} V_{i,j}\left(\|q_i - q_j\|\right). \tag{3}$$

Here the m_i represent masses of objects with positions and momenta $q_i, p_i \in \mathbb{R}^3$. $V(r)$ represents some potential function, for example r^{-1} for gravitational problems and $r^{-12} - r^{-6}$ for molecular dynamics problems, and $\|\cdot\|$ is the Euclidean distance. We would like to integrate these equations for long times where many near collisions (and hence large forces and velocities) may occur, whilst conserving the energy H and the total angular momentum of the system $L = \sum_{i=1}^{N} p_i \times q_i$.

We shall consider here three numerical schemes. The simplest possible is the first-order method

A. Forward (explicit) Euler method (FE)

$$\begin{aligned} \mathbf{p}^{n+1} &= \mathbf{p}^n - \Delta t H_q(\mathbf{p}^n, \mathbf{q}^n), \\ \mathbf{q}^{n+1} &= \mathbf{q}^n + \Delta t H_p(\mathbf{p}^n, \mathbf{q}^n). \end{aligned}$$

The natural partitioning present in (2) suggests the use of partitioned methods [21]. If we combine the backward (implicit) Euler method for one equation, and the forward (explicit) Euler method for the other, we get the following implicit method of order one.

B. Symplectic Euler method (SE)

$$\begin{aligned} \mathbf{p}^{n+1} &= \mathbf{p}^n - \Delta t H_q(\mathbf{p}^{n+1}, \mathbf{q}^n), \\ \mathbf{q}^{n+1} &= \mathbf{q}^n + \Delta t H_p(\mathbf{p}^{n+1}, \mathbf{q}^n). \end{aligned}$$

For systems with separable Hamiltonians, that is those for which we may write $H = T+V$, where $T \equiv T(\mathbf{p})$ and $V \equiv V(\mathbf{q})$, (3) is an example of this case, it turns out that partitioned Runge-Kutta methods may be used to yield explicit symplectic methods — a result which is not true for discretisations of problems with general Hamiltonians. For example, the symplectic Euler method is explicit when applied to problems of this form.

For simplicity, if we now consider the separable case and apply the two-stage Lobatto IIIA-B Runge-Kutta pair (see [18]) we obtain the following second-order explicit symplectic method.

C. Störmer-Verlet method (SV)

$$\begin{aligned} \mathbf{q}^{n+1/2} &= \mathbf{q}^{n-1/2} + \Delta t T_p(\mathbf{p}^n), \\ \mathbf{p}^{n+1} &= \mathbf{p}^n - \Delta t V_q(\mathbf{q}^{n+1/2}). \end{aligned}$$

A form of this method appeared in the molecular dynamics literature [37] many years before anyone realised that its remarkable success in that field was due to the fact that it was in fact a very efficient symplectic method.

This idea of decomposing the Hamiltonian (or equivalently the differential system arising from it) into more than one part turns out to be a good motivation for the class of *splitting* methods, of which symplectic Euler and Störmer-Verlet are two examples. In such methods the whole problem is *split* into simpler problems and each then solved separately. For example, for our Hamiltonian of the form $H = T(\mathbf{p}) + V(\mathbf{q})$ consider the Hamiltonian systems generated by $T(\mathbf{p})$ and $V(\mathbf{q})$ separately

$$\begin{array}{l|l} \dot{\mathbf{p}} = 0 & \dot{\mathbf{p}} = -V_q(\mathbf{q}) \\ \dot{\mathbf{q}} = T_p(\mathbf{p}) & \dot{\mathbf{q}} = 0, \end{array}$$

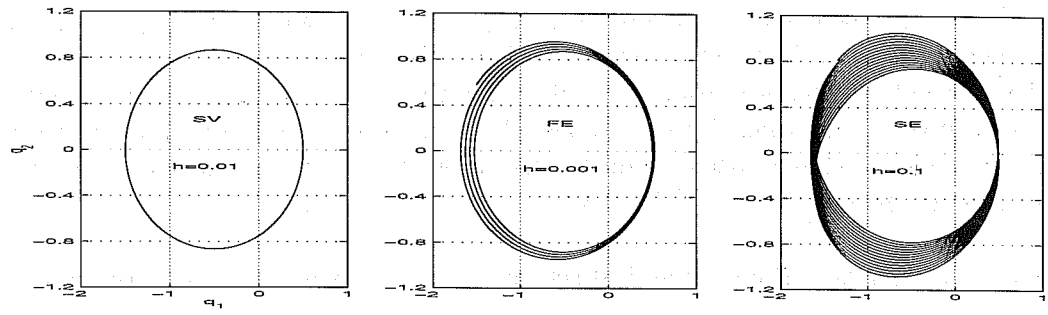

Figure 1: *Kepler trajectories computed with the Störmer-Verlet method (SV), the forward Euler method (FE), and the symplectic Euler method (SE). SV is included as a close approximation to what the true solution looks like. h represents the time step Δt.*

which can be solved exactly

$$\begin{aligned} \mathbf{p}(t) &= \mathbf{p}_0 \\ \mathbf{q}(t) &= \mathbf{q}_0 + T_p(\mathbf{p}_0)t \end{aligned} \quad \Bigg| \quad \begin{aligned} \mathbf{p}(t) &= \mathbf{p}_0 - V_q(\mathbf{q}_0)t \\ \mathbf{q}(t) &= \mathbf{q}_0. \end{aligned}$$

If we now denote the time-t flows of these systems by φ_t^T and φ_t^V respectively, then it can be easily checked that the Symplectic Euler method is simply the composition $\varphi_{\Delta t}^T \circ \varphi_{\Delta t}^V$, and the Störmer-Verlet method $\varphi_{\Delta t/2}^V \circ \varphi_{\Delta t}^T \circ \varphi_{\Delta t/2}^V$. The latter is often called the *Strang splittng* of the problem. Since φ_t^T and φ_t^V are the exact flows for Hamiltonian problems they, and their compositions, are all symplectic mappings. This gives both a quick proof of the symplecticity of these two methods, as well as an introduction to the ideas behind splitting and composition methods.

We shall now use the example of the Kepler (or two-body) problem to demonstrate the behaviour of these methods. The Kepler problem may be written as a Hamiltonian sytem with

$$H(p_1, p_2, q_1, q_2) = \frac{1}{2}(p_1^2 + p_2^2) - \frac{1}{\sqrt{q_1^2 + q_2^2}},$$

so that $V(r) = r$ in (3). The exact dynamics of this system exactly preserve H which represents total energy, as well as the angular momentum given by $L = q_1 p_2 - q_2 p_1$, and also the symplectic structure discussed earlier. In addition, the problem has rotational as well as scaling symmetries, we shall consider the latter presently. In figure 1 we show some trajectories computed with the three methods introduced above. The Störmer-Verlet method is included as a close approximation to how the true solution looks. For the initial data used here the exact solution is an ellipse of eccentricity $e = 0.5$ with the origin at one focus. Notice that the forward Euler trajectory spirals outwards and so does not accurately reproduce the periodic solution to this problem. The symplectic Euler does better in this respect, the numerical solution lies much closer to an ellipse, however it exhibits clockwise precession (the ellipse rotates) about the origin. In figure 2 we look at the growth in trajectory error (computed using the Euclidean norm) and the conservation of Hamiltonian (or energy) for our methods. Note the boundedness of the Hamiltonian error for the symplectic methods, as well as the linear as opposed to quadratic growth in the trajectory error.

These results are summarized in the following table. Note that both the symplectic Euler and Störmer-Verlet methods preserve the angular momentum exactly. The reason being

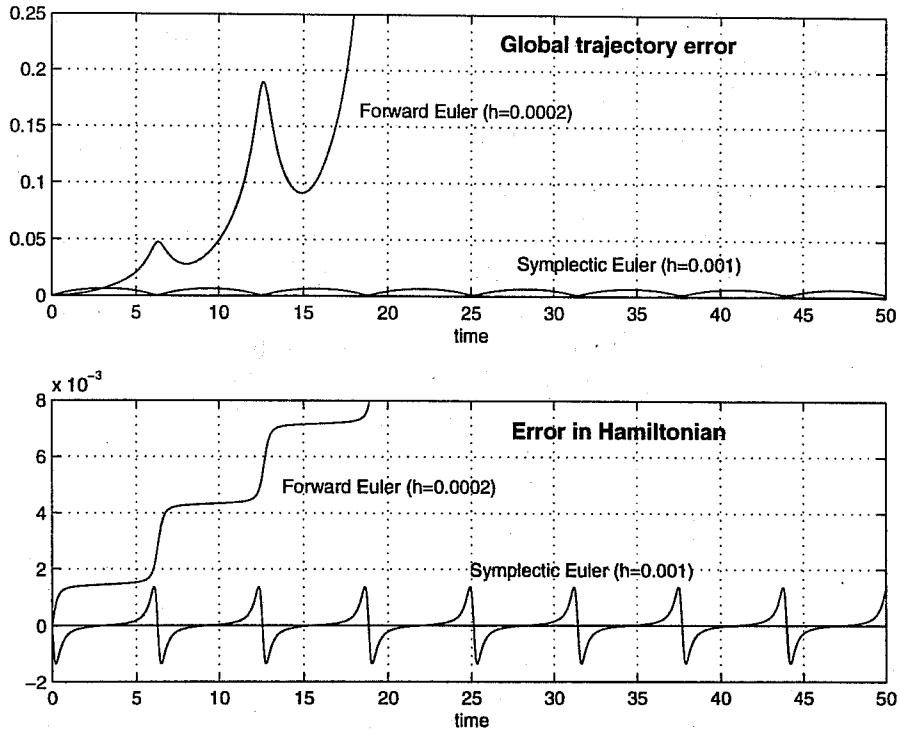

Figure 2: *Errors in trajectory positions for numerical approximations to the Kepler problem. The Störmer-Verlet method results are also plotted with time-step equal to that of the symplectic Euler method, however they are so small it is impossible to distinguish them from the x-axis.*

that symplectic methods often also give exact conservation of quadratic invariants, see [18].

Method	Error in H	Error in L	Global error
FE	$\mathcal{O}(t\Delta t)$	$\mathcal{O}(t\Delta t)$	$\mathcal{O}(t^2\Delta t)$
SE	$\mathcal{O}(\Delta t)$	0	$\mathcal{O}(t\Delta t)$
SV	$\mathcal{O}(\Delta t^2)$	0	$\mathcal{O}(t\Delta t^2)$

See [18, 34] for similar experiments and discussions, as well as proofs and explanations of the apparent superiority of symplectic over non-symplectic methods.

More sophisticated methods, using some of these ideas, have been used to compute the evolution of the solar system for many millions of years. In particular the evolution of the outer planets was computed for a billion years [38], providing numerical confirmation that the motion of Pluto is chaotic.

Note that for problems with close approaches, and hence large forces and velocities, some form of adaptivity often needs to be employed. See the later section on temporal adaptivity and singularities.

3.2 Rigid body motion

We shall now consider the problem of a rigid body with centre of mass fixed at the origin. The body moves according to the Euler equations

$$\begin{aligned}\dot{y}_1 &= (I_2 - I_3)y_2y_3/I_2I_3\\ \dot{y}_2 &= (I_3 - I_1)y_3y_1/I_3I_1\\ \dot{y}_3 &= (I_1 - I_2)y_1y_2/I_1I_2\end{aligned}$$

where (I_1, I_2, I_3) are the moments of inertia about coordinate axes and (y_1, y_2, y_3) the body angular momenta. This is an example of a system which cannot be written in the canonical Hamiltonian form (2). However we may generalize the details of the previous section and write the Euler equations in the form

$$\dot{\mathbf{y}} = \{\mathbf{y}, H\}, \tag{4}$$

where the conserved Hamiltonian function and the bracket operation on functions of $\mathbf{y}$ is given by

$$H(\mathbf{y}) = \frac{1}{2}\left(\frac{y_1^2}{I_1} + \frac{y_2^2}{I_2} + \frac{y_3^2}{I_3}\right), \quad \{F, G\}(\mathbf{y}) = -\mathbf{y}\cdot(\nabla F \times \nabla G).$$

(See [26, 31] for further details of the bracket operation, including the properties it must satisfy.) Following these operations through we can see that

$$\dot{\mathbf{y}} = \mathbf{y} \times \nabla H(\mathbf{y}) \equiv J(\mathbf{y})\nabla H(\mathbf{y}),$$

where $J(\mathbf{y})$ is the skew-symmetric matrix

$$J(\mathbf{y}) = \begin{bmatrix} 0 & -y_3 & y_2 \\ y_3 & 0 & -y_1 \\ -y_2 & y_1 & 0 \end{bmatrix} \tag{5}$$

Since functions of $\mathbf{y}$ also evolve in the same manner as (4), we can obtain the additional conserved quantity of the system $S(\mathbf{y}) = y_1^2 + y_2^2 + y_3^2$, by observing that

$$\frac{d}{dt}S(\mathbf{y}) = \{S, H\}(\mathbf{y}) = -\mathbf{y}\cdot(\mathbf{y} \times \nabla G),$$

which is obviously zero. Notice that we can say further that $\{S, F\} = 0$ for all functions F, and so conservation of S follows from the form of the bracket operation and not the Hamiltonian, a quantity of this type is known as a Casimir invariant. The conservation of S tells us that the motion of our system evolves on the sphere, i.e. we have a differential equation on the two-dimensional manifold S^2 (the two-sphere in $\mathbb{R}^3$), and conservation of H that motion also evolves on an ellipsoid. An ideal numerical scheme will reproduce both of these invariants. For an example of a less than ideal method consider the Forward Euler method, it behaves in a similar manner to how we saw it compute orbits in the Kepler problem. The value of S increases and a computed solution moves out from the sphere on which the initial data sat. In comparison, the implicit midpoint method applied to this problem will exactly conserve both S and H, this is due to the fact that this method exactly conserves quadratic invariants. For a discussion of both the rigid body and other problems of this type see [19].

The special form that J takes, and hence also the bracket operation, means that this problem is of Lie-Poisson type. In particular a Lie-Poisson system associated with the

Lie algebra to the Lie group $SO(3)$ (the group of orthogonal 3×3 matrices with unit determinant). This association with $SO(3)$ makes sense if we notice that the configuration of our rigid body may be given in terms of a rotation from a reference configuration. See [26] (including the front cover) for further details, and [27] for a numerical method which respects this structure.

A review and comparison of various methods for this system may be found in [8].

3.3 Temporal adaptivity and singularity capturing

We shall consider now problems which are invariant under a scaling transformation, what we mean here is that if the dependent and independent variables present in a differential equation are scaled appropriately then the equation remains unchanged. For example consider the problem of one-dimensional motion in a gravitational field (a one-dimensional version of the Kepler problem)

$$\begin{aligned} \dot{r} &= v \\ \dot{v} &= -\frac{1}{r^2}. \end{aligned} \tag{6}$$

This system is left unchanged following the change of variables,

$$t \to \lambda t, \quad r \to \lambda^{2/3} r, \quad v \to \lambda^{-1/3} v,$$

for any arbitrary positive constant λ. Notice that this problem can also be written in canonical Hamiltonian form (2), with Hamiltonian

$$H(r, v) = \frac{v^2}{2} - \frac{1}{r}.$$

A singularity can occur in this system in finite time T. This is called *gravitational collapse* and occurs when a particle falls into the sun. An example of a solution with this property is the following self-similar solution, an important type of solution which is itself invariant under the transformation.

$$\begin{aligned} r &= \left(\frac{9}{2}\right)^{1/3} (T-t)^{2/3} \\ v &= -\left(\frac{2}{3}\right)\left(\frac{9}{2}\right)^{1/3} (T-t)^{-1/3}. \end{aligned} \tag{7}$$

We immediately observe that conventional numerical methods fail (including symplectic) if a fixed time-step is used, due to the singular nature of solutions to this problem. An explicit method will always give a bounded solution, and an implicit method may not have soluble algebraic equations. Some form of adaptivity therefore needs to be used for this problem. More generally, we can further say that adaptive methods fall naturally within the geometric integration framework as fixed mesh methods impose constraints on the solution whereas adaptivity allows the solution and method to evolve together. What we mean here is that if we reparameterize time it is possible for us to derive numerical methods which are themselves invariant under the scaling transformation. We now follow this through for the gravitational collapse problem, and explain what benefits we acheive.

Introduce a map which describes a rescaling of the time variable in terms of a new computational or fictive variable τ, given by

$$\frac{dt}{d\tau} = g(r, v).$$

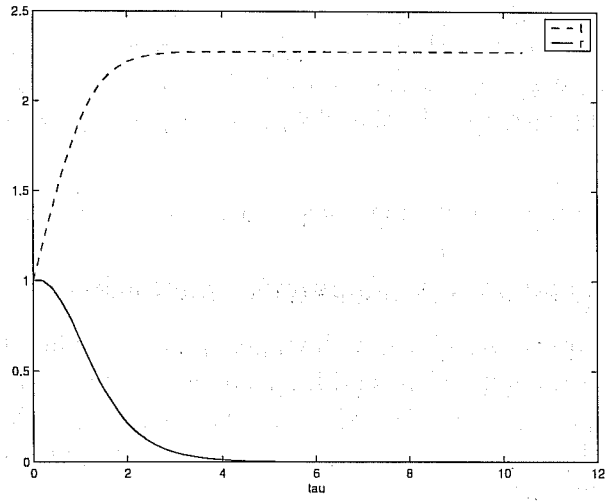

Figure 3: *Convergence properties of t_n and r_n as functions of τ.*

We impose the constraint that $g(\lambda^{2/3}r, \lambda^{-1/3}v) = \lambda g(r,v)$, a suitable choice is $g(r,v) = r^{3/2}$. Our reason for doing this is that our new system is invariant under the scaling transformation with τ *fixed.* Therefore, a numerical discretisation of our new system with fixed computational time-step $\Delta\tau$ is also invariant, in that if (r_n, v_n, t_n) are discrete approximations to $(r(n\Delta\tau), v(n\Delta\tau), t(n\Delta\tau))$, whenever (r_n, v_n, t_n) is a solution of our set of discrete equations induced by the discretisation then $(\lambda^{2/3}r_n, \lambda^{-1/3}v_n, \lambda t_n)$ is also a solution. Under this time transformation (6) rescales to the scale invariant problem

$$\begin{aligned} \frac{dr}{d\tau} &= r^{3/2}v, \\ \frac{dv}{d\tau} &= -\frac{1}{r^{1/2}}, \\ \frac{dt}{d\tau} &= r^{3/2}. \end{aligned} \tag{8}$$

In particular, consider a forward Euler discretisation of (8) with constant step-size $\Delta\tau$.

$$\begin{aligned} r_{n+1} - r_n &= r_n^{3/2} v_n \Delta\tau \\ v_{n+1} - v_n &= -r_n^{-1/2}\Delta\tau \\ t_{n+1} - t_n &= r_n^{3/2}\Delta\tau. \end{aligned} \tag{9}$$

We now look at some results from an implementation of the forward Euler discretisation with initial conditions $r = 1$ and $v = 0$, at (without loss of generality) $t = 1$. The true solution for these initial conditions is not self-similar, but it evolves towards a true self-similar solution as the collapse time T is approached.

In Figure 3 we plot t_n and r_n both as functions of τ. Observe that t_n tends towards the constant value of T_Δ whilst r_n tends to zero. In Figure 4 we present a plot of r_n as a function of t_n in this case. Observe the singular nature of collapse of the solution.

We shall now discuss some theory that explains the excellent qualitative performance of this method. Many additional details may be found in [6].

1. Linear multi-step discretisations of our transformed system (for the above example

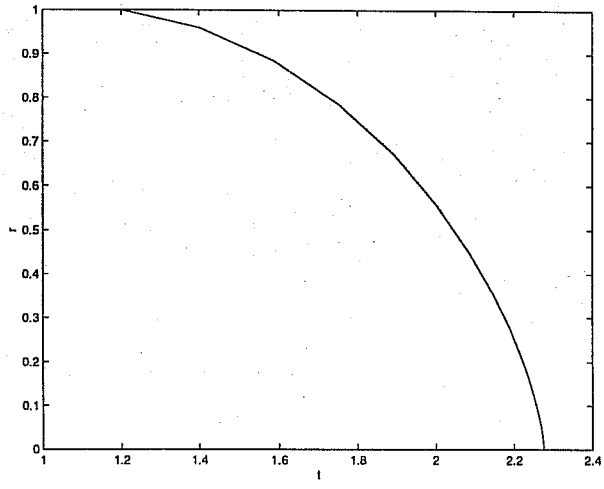

Figure 4: *The collapse of* r *as* $t \to T$.

(8)) have relative local truncation errors which are independent of scale.

2. Global properties of the continuous solution which are derived from scaling invariance may be inherited by the numerical scheme, one example being Kepler's third law, see earlier section.

3. Any continuous self-similar soultions of the problem are uniformly (in time) approximated by discrete self-similar solutions admitted by the numerical method. These discrete solutions also inherit the stability of the continuous ones.

The importance of points 1. and 3. can be seen from the following. Suppose we are computing a solution to a problem in which a singularity is forming, and that the formation is progressively descibed through the action of the scaling group. Our adaptive numerical method will continue to compute with no overall loss in relative accuracy.

The first part of point 3. is best stated via the following theorem.

Theorem. *Let* $u_i(t)$ *(for our collapse problem* $u_1 \equiv r$ *and* $u_2 \equiv v$*) be a self-similar solution of our ordinary differential equation, then there is a discrete self-similar solution* $(u_{i,n}, t_n)$ *of the discrete scheme approximating our rescaled system (for the collapse problem, (8)) such that for all* n

$$u_i(t_n) = u_{i,n}(1 + \mathcal{O}(\Delta\tau^p))$$

where p *is the order of the discretisation and the constant implied in the* $\mathcal{O}(\Delta\tau^p)$ *term does not depend on* n.

The most interesting physical self-similar solutions are those which act as attractors since they determine asymptotic behaviour of more general solutions. The stability result mentioned in point 3. ensures that we are not destroying this property in our numerical method.

If we now return to our gravitational collapse problem we can observe some of these theoretical results when comparing the discrete and true solutions. Our transformed system (8) has the collapsing self-similar solution (from (7))

$$r = Re^{2\mu\tau/3}, \quad v = -Ve^{-\mu\tau/3}, \quad t = T - e^{\mu\tau} \tag{10}$$

where

$$\mu = -\left(\frac{9}{2}\right)^{1/2}.$$

Observe that as $\tau \to \infty$ we have $r \to 0$, $|v| \to \infty$ and $t \to T$, and that $t = T - 1$ at $\tau = 0$. Similarly our numerical scheme (9) admits a discrete collapsing self-similar solution of the form

$$r_n = \hat{R} z^{2n/3}, \quad v_n = -\hat{V} z^{-n/3}, \quad t_n = T_{\Delta\tau} - z^n.$$

Comparing with (10) we see that z is an anologue of $\exp(\mu\Delta\tau)$ if $n\Delta\tau = \tau$. Here $|z| < 1$ so that $r_n \to 0$, $|v_n| \to \infty$ and $t_n \to T_{\Delta\tau}$ as $n \to \infty$, (c.f. [9]). $T_{\Delta\tau}$ is a discrete collapse time which need not necessarily coincide with the true collapse time T, however as $\tau \to \infty$ we have $T_{\Delta\tau} \to T$. Substituting into our forward Euler discretisation we find the values of the constants

$\Delta\tau$	$\hat{R}$	$\hat{V}$	z
0.2	1.46704	1.04761	0.64461
0.1	1.55633	1.07440	0.80584
0.05	1.60298	1.08760	0.89852

notice that in agreement with the theory we have

$$\hat{R} = R(1 + \mathcal{O}(\Delta\tau)), \quad \hat{V} = V(1 + \mathcal{O}(\Delta\tau)), \quad z = e^{\mu\Delta\tau}(1 + \mathcal{O}(\Delta\tau^2))$$

where from (7) we have

$$R = 1.65096, \quad V = 1.100642,$$

and $\exp(\mu\Delta\tau)$ takes the values 0.65425, 0.80886, and 0.89937 for the three choices of $\Delta\tau$ above. See [6] for further results and examples.

3.4 Spatial adaptivity

Partial differential equation problems often involve a complex interaction between temporal and spatial structures. This can take many forms, but a common interaction concerns scalings, so that a change in the temporal scale of the solution is related to a change in the spatial scale. It is possible to capture this behaviour using an adaptive method based upon geometric ideas. We will now describe a general method for adapting the spatial mesh and then show how geometric ideas can naturally be incorporated into it. In an analogous manner to the way in which we constructed an adaptive temporal mesh through a time reparameterization or transformation function, where the time t was described in terms of a differential equation in a fictive variable τ, we can think of a spatial mesh X being a function of a fictive spatial variable ξ such that X satisfies a differential equation in ξ. Here we will assume that this function has a high degree of regularity (i.e. we progress beyond thinking of a mesh as a piece-wise constant function of ξ.) The crucial idea behind generating such a mesh is that of *equidistribution* of an appropriate *monitor* function.

The approach we use here in one-dimension is based on the framework which is developed in [23]. It is possible to use similar ideas in higher dimensions, see [24], but this is naturally a more complex process. Equidistribution can be loosely thought of as a process for changing the *density* of the mesh points in response to the solution (in contrast to Lagrangian methods which tend to change the mesh points themselves.) Our discussion will be confined to the one-dimensional case.

We define the physical mesh, that is the mesh upon which the physical problem is posed, in terms of a mesh function $X(\xi, t)$ which maps a computational (fictive) coordinate $\xi \in [0, 1]$

onto a physical coordinate (which we assume without loss of generality to be in $[0,1]$) such that

$$X\left(\frac{j}{N},t\right) = X_j(t), \qquad j = 0,\ldots,N.$$

Therefore our $N+1$ mesh points $X_j(t)$, which are permitted to vary with time, are simply the image of a uniform *computational* mesh under a time dependent mesh function.

We now introduce a monitor function $M(x,u,u_x)$ which classically represents some measure of computational difficulty in the problem, and invoke the principle of equidistribution by defining our mesh function X through the relation

$$\int_0^X M\,dx = \xi \int_0^1 M\,dx. \tag{11}$$

Differentiating with respect to ξ we see that the mesh-density X_ξ satisfies the equation

$$X_\xi = \int_0^1 M\,dx/M, \tag{12}$$

so that the mesh density is inversely proportional to M. The equation above may be differentiated again to give the following partial differential equation for the mesh — referred to as MMPDE1 (moving mesh partial differential equation 1)

$$(MX_\xi)_\xi = 0.$$

This equation may then be solved for the mesh by discretising the function X appropriately [23]. In practice this can lead to an unstable system and many related partial differential equations have been derived to stabilise this process — with details given in [23]. An example of such a stabilisation is MMPDE6 given by

$$\varepsilon X_{t\xi\xi} = -(MX_\xi)_\xi$$

where ε is a small relaxation parameter. A further advantage of this approach is that is allows the use of an initially uniform mesh. To solve the original partial differential equation, both the partial differential equation for the mesh function X and the partial differential equation for $u(x,t)$ are discretised. (It often pays to use a high order discretisation in both cases). One of the mesh equations may then be coupled with the original PDE, giving a new system.

The new coupled system may or may not inherit the qualitative features of the original problem. The geometric integration viewpoint is to produce a mesh in which the mesh equation inherits as many qualitative features as possible. As an important example, we may seek a mesh so that the new system has the same scaling invariances as the original. As the mesh is governed by the monitor function M this problem reduces to that of choosing M such that the coupled system is invariant with respect to the same transformation group as the original equation. By doing this we ensure that all of the scaling symmetry structure of the underlying partial diferential equation will be inherited by the resulting numerical method. It is possible to do this for a wide variety of problems with relatively simple choices of M leading to some elegant scaling invariant methods.

We shall now look at a specific example.

3.4.1 Singularities in the nonlinear Schrödinger equation (NLS)

The radially symmetric solutions of the cubic nonlinear Schrödinger equation satisfy the following partial differential equation

$$iu_t + u_{xx} + \frac{d-1}{x}u_x + u|u|^2 = 0. \tag{13}$$

Where d is the dimension of the problem and x is the distance from the origin. If $d \geqslant 2$ this problem has solutions which blow-up so that they develop singularities at the origin in a finite time T (in a manner similar to that of gravitational collapse) so that the solution tends to infinity in an increasingly narrow (in space) peak. This partial differential equation is unitary, and can be written in Hamiltonian form. During the evolution the following are invariant quantities

$$\int_0^\infty |u|^2 x^{d-1}\,dx \quad \text{and} \quad \int_0^\infty \left(|u_x|^2 - \frac{1}{2}|u|^4\right) x^{d-1}\,dx. \tag{14}$$

The nonlinear Schrödinger equation is a model of the modulational instability of water waves and plasma waves, and is important in studies of nonlinear optics where the refractive index of a material depends upon the intensity of a laser beam. In the latter case, blow-up corresponds to a self-focusing of the wave. Furthermore, the one-dimensional ($d = 1$) form of (13), is integrable and has many symmetries and invariants. Its numerical solution can exploit these by using geometric integration methods and this is discussed from a numerical viewpoint in [28]. A general discussion of the singularity formation of the NLS equation is given in [35].

We now briefly discuss a numerical method to solve (13) when $d \geqslant 2$ which is based upon geometrical ideas and which is very effective at computing the blow-up solutions. Details of this method are given in [3]. This method is based on preserving the scaling symmetries of the problem rather than either of the two invariant quantities (14). In particular (13) is invariant under the action of either of the transformations

$$t \to \lambda t, \quad x \to \lambda^{1/2} x, \quad u \to \lambda^{-1/2} u \tag{15}$$

and

$$u \to e^{i\varphi} u, \quad \varphi \in \mathbb{R}.$$

We seek a numerical method which inherits both of these symmetries, and achieve this through the use of adaptivity of both the temporal and spatial meshes.

The temporal and spatial adaptivity used for this example are given by solving the following equations

$$\frac{dt}{d\tau} = \frac{1}{|u(0,t)|^2},$$

coupled with MMPDE6. The choice of monitor function

$$M = |u|^2$$

results in a combined system for the mesh and the solution which is invariant under the full set of scaling transformations.

The resulting coupled system is discretised in space using a collocation method and the resulting ODE system is then solved using a BDF discretisation [21]. The resulting method has proved very effective at computing singular solutions using only a modest number

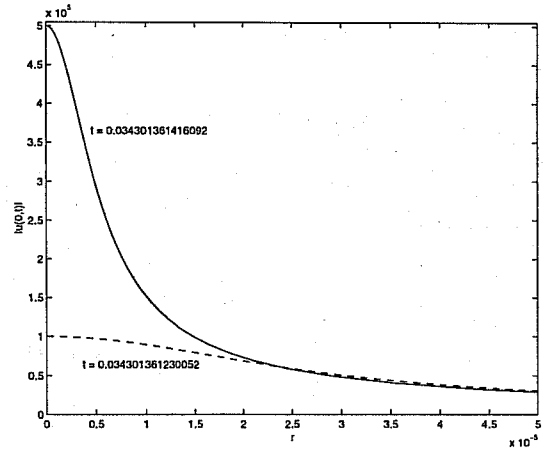

Figure 5: *The solution when* $|u(0,t)| = 100000$ *and* 500000

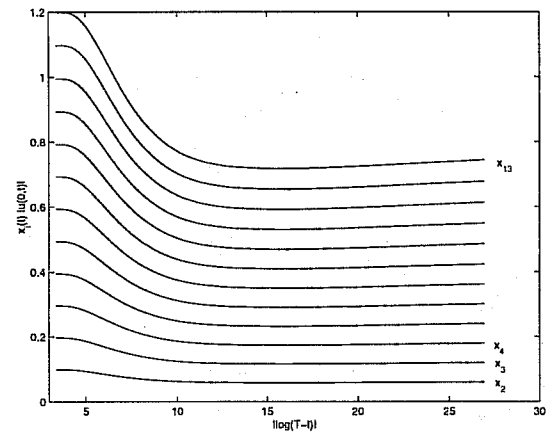

Figure 6: *The scaled mesh* $X_i(t)|u(0,t)|$

$(N = 81)$ of mesh points in the computational domain. The computations have revealed much new structure in the problem [4].

We now present the results of a computation which evolves towards the singular blow-up self-similar solution which has a monotone profile. Figure 5 shows two solutions taken when $d = 3$ with initial data $u(0,x) = 6\sqrt{2}\exp(-x^2)$ if $0 \leqslant x \leqslant 5$, and $u(0,x) = 0$ if $x > 5$. In this case the estimated value of T is $T = 0.0343013614215$. These two solutions are taken close to the blow-up time when the amplitude of $|u|$ is around 10^5 and the peak has width around 10^{-5}. Observe that the resolution of the peak is very good, indicating that the mesh points are adapting correctly.

In figure 6 we present a plot of $X_i(t)|u(0,t)|$ as a function of $\log(T-t)$ for a range in which u varies from 100 to 500000. According to (15) the quantity ux is an invariant of the scaling transformation and is therefore also a constant for a self-similar solution. Observe that in the computations these values rapidly evolve towards constants, demonstrating that the mesh is evolving in a self-similar manner.

Thus, as in the case of gravitational collapse, adaptivity has led to an attracting self-similar

solution being precisely recreated by the numerical solution and the mesh.

4 Case studies II: meteorological model problems

We now consider two meteorological problems for which a geometric integration based numerical approach to their solution looks promising.

4.1 Semi-geostrophic equations and frontogenesis

The three-dimensional Boussinesq equations of semi-geostrophic theory on a plane with constant coriolis force f may be written in the form (for many further details see [22, 12, 13])

$$\left.\begin{aligned} \frac{Du_g}{Dt} - fv + \frac{\partial \varphi}{\partial x} &= \frac{Du_g}{Dt} - f(v - v_g) = 0, \\ \frac{Dv_g}{Dt} + fu + \frac{\partial \varphi}{\partial y} &= \frac{Dv_g}{Dt} + f(u - u_g) = 0, \end{aligned}\right\} \tag{16}$$

$$\begin{aligned} \frac{D\theta}{Dt} &= 0, \\ \nabla_x \cdot \mathbf{u} &= 0, \\ \nabla_x \varphi &= (fv_g, -fu_g, g\frac{\theta}{\theta_0}). \end{aligned} \tag{17}$$

Here (u_g, v_g) is the geostrophic wind, θ the potential temperature, and φ the geo-potential. The energy integral E defined by

$$E = \int_D \left(\frac{1}{2}(u_g^2 + v_g^2) - \frac{g\theta z}{\theta_0} \right) dx\, dy\, dz$$

is an invariant of this set of equations. This equation set is of interest for many reasons, one being that it allows the study of idealised atmospheric weather fronts. That is, just as for the nonlinear Schrödinger equation it admits solutions which form singularities in finite time.

It is usual to define a coordinate transformation from (x, y, z) coordinates to isentropic geostrophic momentum coordinates

$$\mathbf{X} \equiv (X, Y, Z)^T = \left(x + \frac{v_g}{f}, y - \frac{u_g}{f}, \frac{g\theta}{f^2\theta_0} \right)^T. \tag{18}$$

In a similar manner to the previous section we can think of (X, Y, Z) as being (fictive) computational coordinates introduced in earlier sections, (18) then describes the evolution of a spatial mesh. In terms of these new coordinates (16) and (17) transform to

$$\frac{D\mathbf{X}}{Dt} = \mathbf{u}_g \equiv (u_g, v_g, 0)^T, \tag{19}$$

and hence the motion in these new coordinates is exactly geostrophic, as well as nondivergent $\nabla_X \cdot \mathbf{u}_g = 0$. A numerical method based on (19) will perform in an adaptive way — a Lagrangian form of mesh adaptivity where the mesh is moved at exactly the speed of the underlying velocity field.

The ratio of volume elements in dual space to that of physical space is given by

$$q = \frac{\partial(X, Y, Z)}{\partial(x, y, z)}.$$

This relates the scaling of the spatial mesh to the computational mesh. The expression q defines a consistent form of the Ertel potential vorticity (PV) in SG theory, satisfying

$$\frac{Dq}{Dt} = 0.$$

It is possible to write our coordinate transformation as $\mathbf{X} = \nabla_x P$ where

$$P(\mathbf{x}) = \frac{\varphi}{f^2} + \frac{1}{2}(x^2 + y^2).$$

Hence q, the PV, is equivalently the determinant of the Hessian of P with respect to the coordinates $\mathbf{x}$,

$$q = \det(\mathrm{Hess}_x(P)).$$

Also, $\mathbf{x} = \nabla_{\mathbf{X}} R$, where $P(\mathbf{x})$ and $R(\mathbf{X})$ are a pair of Legendre transforms related by

$$P + R = \mathbf{x} \cdot \mathbf{X}.$$

We can now introduce a streamfunction for the geostrophic velocities,

$$\Psi = f^2 \left(\frac{1}{2}(X^2 + Y^2) - R(\mathbf{X}) \right), \quad (u_g, v_g) = \frac{1}{f} \left(-\frac{\partial \Psi}{\partial Y}, \frac{\partial \Psi}{\partial X} \right). \tag{20}$$

Defining ρ (the pseudo-density) to be

$$\rho \equiv q^{-1} = \det(\mathrm{Hess}_X(R)), \tag{21}$$

it can be shown that

$$\frac{D_X \rho}{Dt} \equiv \frac{\partial \rho}{\partial t} - \frac{1}{f} \frac{\partial(\rho, \Psi)}{\partial(X, Y)} = 0, \tag{22}$$

It is now possible to compute the evolution of this system using the following procedure,

1. given an initial distribution of pseudo-density solve the nonlinear elliptic equation of Monge-Ampère type (21) for R,
2. using the streamfunction (20) compute a new velocity field (u_g, v_g),
3. advect the pseudo-density distribution using (22) and return to start.

We thus have two distinct numerical problems to solve. The first being the computation of a solution to the Monge-Ampère equation (21). This is obviously linked to determining the coordinate transformation (18), since for a given R we have $\mathbf{x} = \nabla_{\mathbf{X}} R$, and hence fits in well with our discussions of coordinate transformations and adaptivity earlier. The second numerical challenge is that of solving the advection equation (22). We will now show that this also has a nice geometric structure, and then return to the adaptivity connection.

4.1.1 Hamiltonian formulations

We now consider Hamiltonian formulations for this problem, Roulstone and Norbury [32] discuss two Hamiltonian formulations of the semi-geostrophic equations. The first, a canonical (infinite-dimensional extension of (2)) representation of the equations of motion (19), with Hamiltonian functional

$$\mathscr{H}[\mathbf{X}] = f \int d\mathbf{a} \left(\frac{1}{2}(X^2(\mathbf{a}) + Y^2(\mathbf{a})) - R(\mathbf{X}(\mathbf{a})) \right),$$

where $\mathbf{a}$ is a Lagrangian particle labelling coordinate. The standard canonical Poisson bracket is given by

$$\{\mathscr{F}, \mathscr{G}\}_c = \int d\mathbf{a} \left(\frac{\delta \mathscr{F}}{\delta X(\mathbf{a})} \frac{\delta \mathscr{G}}{\delta Y(\mathbf{a})} - \frac{\delta \mathscr{F}}{\delta Y\mathbf{a})} \frac{\delta \mathscr{G}}{\delta X(\mathbf{a})} \right).$$

As for the rigid body bracket (3.2), refer to [26, 31] and [32] for further details of this bracket operation. It is possible to prove conservation of PV (equivalently pseudo-density) along trajectories by demonstrating that

$$\{q, \mathscr{H}\}_c = 0.$$

Again following [32] we may write our advection equation (22) in Hamiltonian form. Using our previous Hamiltonian, this time evaluated in phase space solely as a functional of ρ. That is,

$$\mathscr{H}[\rho] = f \int d\mathbf{X}\ \rho(\mathbf{X}) \left(\frac{1}{2}(X^2 + Y^2) - R(\mathbf{X}) \right), \quad \frac{\delta \mathscr{H}}{\delta \rho} = f^2 \left(\frac{1}{2}(X^2 + Y^2) - R \right) \equiv \Psi.$$

We are now in a position to write the equations of motion (22) as

$$\frac{\partial \rho(\mathbf{X})}{\partial t} = \{\rho(\mathbf{X}), \mathscr{H}\}, \tag{23}$$

where the noncanonical Poisson bracket (see [32, 26, 31]) is given by

$$\{\mathscr{F}, \mathscr{G}\} = \int_\Gamma d\mathbf{X} \frac{\delta \mathscr{F}}{\delta \rho(\mathbf{X})} \left(\frac{\partial \left(\rho(\mathbf{X}), \frac{\delta \mathscr{G}}{\delta \rho(\mathbf{X})} \right)}{\partial (X, Y)} \right).$$

Note that in these coordinates, and with this bracket, the pseudo-density becomes a Casimir invariant of the system, $\{\rho, \mathscr{F}\} = 0$ for all functionals $\mathscr{F}(\rho)$, (c.f. the quantity S in the rigid body problem).

The geometric integration problem of numerically integrating these equations whilst preserving the pseudo-density or potential vorticity along the flow turns out to be intimately related to preserving the Hamiltonian (or Poisson bracket) structure of the problem. See [32] for more details, and also [27, 30] for some applications to similar problems where explicit methods capturing the Hamiltonian structure and the Casimir invariants are derived.

4.1.2 Links with moving mesh theory

We now take a closer look at the coordinate transformation from physical to geostrophic or dual coordinates, we also choose to sometimes use the term computational coordinates for X since these are the variables in which computing will be carried out. Recall from earlier we had

$$\mathbf{X} \equiv (X, Y, Z) = \left(x + \frac{v_g}{f}, y - \frac{u_g}{f}, \frac{g\theta}{f^2\theta_0} \right)^T,$$

and

$$q = \frac{\partial(X, Y, Z)}{\partial(x, y, z)} = \det(\mathrm{Hess}_x(P)), \tag{24}$$

we shall now show some links with the theory of moving mesh partial differential equations.

It is possible to write the continuous form of the first one-dimensional moving mesh partial differential equation (MMPDE) in the form (c.f. (12))

$$\frac{\partial x}{\partial \xi} = \frac{1}{M}$$

where $M(x, u)$ is our monitor function. Notice the similarity with (24) if we take $M = q$, and identify the computational coordinates X and ξ. In particular in one-dimension we simply have that $M = P_{xx}$.

In three dimensions the Russell *et al* approach [24] to constructing coordinate transformations ($\xi = \xi(\mathbf{x}, t)$) is to minimize the following integral

$$I[\xi] = \frac{1}{2} \int \sum_{i=1}^{3} \left(\nabla \xi^i \right)^T G_i^{-1} \nabla \xi^i \, d\mathbf{x},$$

where the G_i are monitor functions, three by three symmetric positive definite matrices (concentrates mesh points in regions where G_i is large). The Euler-Lagrange equations for which are

$$-\frac{\delta I}{\delta \xi^i} = \nabla \cdot \left(G_i^{-1} \nabla \xi^i \right) = 0, \quad i = 1, 2, 3.$$

But now notice what happens when we take our monitor functions to be equal $G_i \equiv G$ and

$$G = \mathrm{Hess}_x(P).$$

For a start the determinant of our monitor function is simply the potential vorticity, and one possible solution to the Euler-Lagrange equations is $\xi = \nabla_x P$, since then (using the symmetry of the Hessian if necessary),

$$G^{-1} \nabla \xi^i = \mathbf{e}_i, \quad i = 1, 2, 3; \qquad \mathbf{e}_1 = (1, 0, 0)^T, \text{ etc.}$$

We have thus shown a link between the usual analytical transformation found in the literature and our moving mesh adaptivity ideas discussed in previous sections. A key point to take on board from these is that the equations governing the mesh transformation should be solved to high order, i.e. a smooth mesh should be used. This contrasts with the piecewise constant mesh transformation discussed in [12], as well as the geometric method (a numerical method based on the piecewise constant construction, see [10]).

We hope to employ some of the geometric integration ideas discussed in this paper to the semi-geostrophic equations, with the aim of obtaining the superior results we observed for the nonlinear Schrödinger, and other equations.

4.2 Calculating Lyapunov exponents

Weather forecasting makes *prediction ensembles* to see how reliable a forecast is. This involves discretising the underlying partial differential equations in space to get a system of ordinary differential equations, then looking for the p largest modes of error growth of this system. A systematic way of finding such modes is to calculate Lyapunov exponents of the system.

The calculation of Lyapunov exponents is a natural candidate for a geometric integration based approach as it involves integrating matrix ordinary differential equations which require the preservation of structural properties of the matrices. An interesting algorithm to do this was proposed in [15] and involved integrating systems of equations defining orthogonal matrices. An alternative procedure [20] is to solve the system

$$\dot{Y} = A(t)Y, \quad Y \in M^{n\times p}$$

and find a singular value decomposition (see [36]) of Y using

$$Y = U(t)S(t)V(t),$$

where U is an $n \times p$ matrix with orthogonal columns, V is a $p \times p$ matrix with orthogonal columns and S is a diagonal $p \times p$ matrix of singular values. The growth rates of the dominant modes can then be calculated via the Lyapunov exponents

$$\lambda_i = \lim_{t\to\infty} \left[\frac{1}{t} log S_{ii}(t)\right].$$

Essential to this calculation is determining the matrices U and V. An efficient way to proceed is to determine ordinary differential equations for U and V which typically take the form

$$\dot{U} = AU + U(H - U^T AU) \tag{25}$$

where H is a derived $p \times p$ matrix and U the $n \times p$ matrix with orthogonal columns. Equation (25) is a naturally arising evolutionary system in which keeping the columns of U orthogonal is important for the accuracy of the estimates of the Lyapunov exponents. Conventional integrators will not do this easily, however this structure is amenable to methods based on the Lie group invariance of such systems [25]. The geometric integration approach is to decompose U as a product of Householder reflections [36] and solve the ordinary differential equations that define the reflections. The advantage of using such a procedure for (25) is that it has very efficient estimates (exponential convergence) of subspaces to spaces spanned by the fastest growing modes, although great care needs to be taken when singular values coalesce.

5 Conclusion

We have demonstrated in this paper that the consideration of qualitative properties in ordinary and partial differential equations is important when designing numerical schemes. We have given some examples of general methods and techniques which may be employed to capture geometric features in discretisations of continuous problems. Some theory as well as examples have been used to demonstrate the possible advantages which the geometric integration approach to numerical analysis may yield. Methods applied to problems with Hamiltonian structure, singularity formation, and evolution on manifolds have been described with the view to discussing some problems arising in meteorology

and numerical weather prediction. Some ideas on how these methods may be adapted and used for meteorological problems in the future have been briefly discussed, and work in this area is ongoing.

References

[1] V.I. Arnold, *Mathematical Methods of Classical Mechanics.* Springer-Verlag, New York, (1998).

[2] G.I. Barenblatt, *Scaling, self-similarity and intermediate asymptotics.* CUP, (1996).

[3] C.J. Budd, S. Chen and R.D. Russell, *New self-similar solutions of the nonlinear Schrödinger equation with moving mesh computations.* J. Comp. Phys., **152**, (1999), pp. 756–789.

[4] C.J. Budd, *Asymptotics of new blow-up self-similar solutions of the nonlinear Schrödinger equation.* University of Bath Mathematics preprint 00/20, (2000).

[5] C.J. Budd and A. Iserles (editors), *Geometric integration: numerical solution of differential equations on manifolds.* Phil Trans. Roy. Soc. Lond. A., **357**, (1999), pp. 943–1133.

[6] C.J. Budd, B. Leimkuhler and M.D. Piggott, *Scaling invariance and adaptivity.* University of Bath Mathematics preprint 99/18, (1999).

[7] C.J. Budd and M.D. Piggott, *The geometric integration of scale invariant ordinary and partial differential equations.* University of Bath Mathematics preprint 00/05, (2000).

[8] S.R. Buss, *Accurate and efficient simulations of rigid-body rotations.* J. Comp. Phys., **164**, (2000), pp. 377–406.

[9] Y.G. Chen, *Asymptotic behaviours of blowing-up solutions for finite difference analogue of* $u_t = u_{xx} + u^{1+\alpha}$. J. Fac. Sci. Univ. Tokyo; SecIA, Math., **33**, (1986), pp. 541–574.

[10] S. Chynoweth, *The semi-geostrophic equations and the Legendre transform.* Ph.D thesis, University of Reading, UK., (1987).

[11] M.J.P. Cullen, J. Norbury, and R.J. Purser, *Generalised Lagrangian solutions for atmospheric and oceanic flows.* SIAM J. Appl. Math., **51**, No. 1, (1991), pp. 20–31.

[12] M.J.P. Cullen and R.J. Purser, *An extended Lagrangian theory of semi-geostrophic frontogenesis.* J. Atmos. Sci., **41**, No. 9, (1984), pp. 1477–1497.

[13] M.J.P. Cullen and R.J. Purser, *Properties of the Lagrangian semi-geostrophic equations.* J. Atmos. Sci., **46**, No. 17, (1987), pp. 2684–2697.

[14] M. Cullen, D. Salmond and P. Smolarkiewicz, *Key numerical issues for the development of the ECMWF model.* (2000), this workshop.

[15] L. Dieci, R.D. Russell and E.S. Van Vleck, *On the computation of Lyapunov exponents for continuous dynamical systems.* SIAM J. Numer. Anal., **34**, No. 1, (1997), pp. 402–423.

[16] V. Dorodnitsyn, *Noether-type theorems for difference equations.* IHES/M/98/27, Bures-sur-Yvette (France), (1998).

[17] P. Grindrod, *Patterns and waves.* Oxford University Press, New York, (1991).

[18] E. Hairer, *Numerical geometric integration.* Unpublished lecture notes, (1999), available on http://www.unige.ch/math/folks/hairer/.

[19] E. Hairer, *Geometric integration of ordinary differential equations on manifolds.* to appear, BIT, (2000).

[20] R. Hauser, *Private communication.* (2000).

[21] E. Hairer, S.P. Nørsett and G. Wanner, *Solving ordinary differential equations I.* 2nd edition, Springer series in computational mathematics **8**, Springer-Verlag, Berlin, (1993).

[22] B.J. Hoskins, *The geostrophic momentum approximation and the semi-geostrophic equations.* J. Atmos. Sci., **32**, No. 2, (1975), pp.233–242.

[23] W. Huang, Y. Ren and R.D. Russell, *Moving mesh partial differential equations (MMPDES) based on the equidistributional principle.* SIAM J. Numer. Anal. **31**, no. 3, (1994), pp. 709–730.

[24] W. Huang and R.D. Russell, *A high dimensional moving mesh strategy.* Appl. Numer. Math., **26**, (1999), pp. 998–1015.

[25] A. Iserles, H.Z. Munthe-Kaas, S.P. Nørsett and A. Zanna, *Lie-group methods.* Acta Numerica (2000), pp. 215–365.

[26] J.E. Marsden and T.S. Ratiu, *Introduction to mechanics and symmetry.* Springer-Verlag, (1994).

[27] R.I. McLachlan, *Explicit Lie-Poisson integration and the Euler equations.* Phys. Rev. Lett., **71**, (1993), pp. 3043–3046.

[28] R.I. McLachlan, *Symplectic integration of Hamiltonian wave equations.* Numer. Math., **66**, (1994), pp. 465–492.

[29] R.I. McLachlan and G.R.W. Quispel, *Six lectures on the geometric integration of ODEs.* unpublished.

[30] R. McLachlan, I. Szunyogh and V. Zeitlin, *Hamiltonian finite-dimensional models of baroclinic instability.* Phys. Lett. A, **229**, (1997), pp. 299–305.

[31] P. Olver, *Applications of Lie Groups to Differential equations.* Springer, New York, (1986).

[32] I. Roulstone and J. Norbury, *A Hamiltonian structure with contact geometry for the semi-geostrophic equations.* J. Fluid. Mech., **272**, (1994), pp. 211–233.

[33] A. Samarskii, V. Galaktionov, S. Kurdyumov and A. Mikhailov, *Blow-up in quasilinear parabolic equations.* Walter de Gruyter, (1995).

[34] J.M. Sanz-Serna and M. Calvo, *Numerical Hamiltonian problems.* Chapman and Hall, London, (1994).

[35] C. Sulem and P-L Sulem, *The nonlinear Schrödinger equation.* Applied Mathematical Sciences, **139**, Springer, (1999).

[36] L.N. Trefethen and D. Bau III, *Numerical linear algebra.* SIAM, (1997).

[37] L. Verlet, *Computer "experiments" on classical fluids. I. Thermodynamic properties of Lennard-Jones molecules.* Phys. Rev., **159**, (1967), pp. 98–103.

[38] J. Wisdom and M. Holman, *Symplectic maps for the N-body problem.* Astron. J., **102**, (1991), pp. 1528–1538.